Particles Floating on a Moving Fluid: A Dynamically Comprehensible Physical Fractal

John C. Sommerer and Edward Ott

Measurements of the local dynamics on the surface of a fluid undergoing complicated motion allow prediction of the measured fractal dimension of an aggregate of passive, floating tracers. This realization of a strange attractor in physical space is a rare instance where there is a firm quantitative connection between the dimension of an experimentally observed fractal spatial pattern and the process producing it.

Fractals are scale-invariant geometric objects; any piece of a fractal, appropriately magnified, resembles the whole, at least statistically. Such geometric figures are characterized by a dimension which, unlike that of a familiar Euclidean figure, is generally not an integer (*1*). Many physical processes have been shown to produce phenomena that, while not scale-invariant in an absolute mathematical sense, are self-similar over a very wide range of scales [for many examples, see (*2–4*)]. Such approximate, or physical fractals are also characterized by the noninteger dimension of the corresponding mathematical fractal. Examples of physical fractals frequently discussed are clouds, coastlines, crack profiles, electrical discharges, and aggregates formed by diffusion-limited processes.

Although physical fractal spatial patterns are frequently observed, a quantitative connection between the measured numerical value of the fractal dimension and the underlying physics of the process has largely been lacking (*5*). This lack of connection, while not reducing the utility of fractals for phenomenological characterization, has led to skepticism about the ultimate meaningfulness of fractal descriptions in physics (*6–8*).

On the other hand, the mathematical fractals that appear as strange attractors of nonlinear systems have dimensions that are closely related to the dynamics of the system. The information dimension of a strange attractor can be predicted on the basis of the Lyapunov exponents of the system. (Roughly speaking, the information dimension is the fractal dimension of the highest density regions of the strange attractor; see Eq. 5 for a precise definition.) The Lyapunov exponents describe the tracking of typical neighboring trajectories, and are fundamental quantities that, for example, define whether or not a system is chaotic. However, the strange attractor of a chaotic system is an abstract geometric object inhabiting the phase space of the system as opposed to the fractals of interest here, which inhabit the physical configuration space and can in principle be seen "by eye."

We have developed an experiment that produces physical fractal spatial patterns on the surface of a moving fluid. By considering the movement of passive tracers on the surface of the fluid as resulting from a random dynamical map, we identify the phase space of the dynamical system with the physical space of the fluid surface. We can measure Lyapunov exponents for the map, and can predict the geometric fractal dimension exhibited by the aggregate of tracers. These results constitute (i) the experimental realization of a strange attractor in physical space, (ii) a rare quantitative connection between the dimension of a specific experimental fractal spatial pattern and the underlying physical process, and (iii) a demonstration that the theory of random maps is a useful model of complicated fluid motions. In particular, we quantitatively relate the measured Lyapunov exponents of the particle trajectories to the dimension of the observed fractal spatial pattern. Thus, we establish the dynamical origin of the fractal pattern. We believe that similar processes may underlie many other naturally occurring fractal spatial patterns. If so, the observation of fractal properties can provide insight into underlying physical processes, in addition to phenomenological characterization.

Theoretical background. In this section, we review aspects of dynamical systems theory relevant to the determination of fractal dimensions. We will consider two-dimensional, discrete-time dynamical systems (maps) of the form

$$x_{n+1} = F(x_n, n) \tag{1}$$

where x denotes a point in the plane, and n denotes the time step. Two cases can be distinguished: the standard theory of dynamical systems deals with the case where F is independent of n; and the theory of random maps, which deals with the case where for each value of n, the map F is chosen at random from a family of maps according to some rule. Further, we are interested in the situation where F is not area-preserving in the plane, and in particular where the image of a tiny area typically shrinks on repeated applications of the system in Eq. 1:

$$\alpha \equiv \lim_{n\to\infty} \frac{1}{n} \ln\left[\frac{\text{area}(R_n)}{\text{area}(R_0)}\right] < 0 \tag{2}$$

where R_0 is an initial small region at time zero, and R_n is the region it maps to at time n. The quantity α is referred to as the dissipation of the system, and should not be confused with the friction-induced damping of velocity in a viscous flow.

The relative stability of typical trajectories described by Eq. 1 is measured in terms of two Lyapunov exponents. The largest Lyapunov exponent, λ_1, is the growth rate of a generic infinitesimal vector giving the displacement between two infinitesimally separated points x_n and $x_n + \delta\xi_n$. For a typical such vector $\delta\xi_0$ at an initial point x_0 (with infinitesimal length $\|\delta\xi_0\|$), the largest Lyapunov exponent is defined as

$$\lambda_1 \equiv \lim_{n\to\infty} \frac{1}{n} \ln \frac{\|\delta\xi_n\|}{\|\delta\xi_0\|} \tag{3a}$$

where the infinitesimal displacement vector at time step n, $\delta\xi_n$, is given by the equation of variations associated with the system (Eq. 1):

$$\delta\xi_{n+1} = \mathbf{DF}(x_n) \cdot \delta\xi_n \tag{3b}$$

The matrix $\mathbf{DF}(x)$ is the Jacobian derivative of F evaluated at the point x. The smaller Lyapunov exponent, λ_2, is defined in terms of Eqs. 2 and 3 by

$$\lambda_2 \equiv \alpha - \lambda_1 \tag{4}$$

Geometrically, the Lyapunov exponents can be interpreted as follows. Given an initial infinitesimal circle of radius δr, for very large n the image of the circle under $F^{(n)}$ will be an ellipse of semimajor and semiminor axes of the order of $\delta r \exp(n\lambda_1)$ and $\delta r \exp(n\lambda_2)$, respectively.

A system is defined to be chaotic if $\lambda_1 > 0$, in which case typical nearby trajectories will diverge from one another exponentially fast. However, if $\alpha < 0$, a cloud of initial conditions iterated together under Eq. 1 must eventually occupy a set of arbitrarily small area. Such a spatially distributed, zero-area set on which neighboring trajectories diverge from one another exponentially fast is referred to as a strange attractor; it is a fractal with dimension less than two (and hence, zero area). In the standard

J. C. Sommerer is at the M. S. Eisenhower Research Center, The Johns Hopkins University Applied Physics Laboratory, Laurel, Maryland 20723. E. Ott is in the Departments of Electrical Engineering and Physics, The University of Maryland, College Park, MD 20742.

case, where F is independent of n, the strange attractor is a fixed object in the phase space, and can be visualized by following a single trajectory for a long time (this is the usual procedure for producing the familiar computer graphics of strange attractors). In the case of random maps such as we will consider here, however, the strange attractor changes shape and position in phase space from iteration to iteration, and can only be visualized by simultaneously following a cohort of trajectories.

A "natural probability measure" is supported on the strange attractor. In the case of random maps, the natural measure of a region in phase space (on a given value of n) is defined as the proportion of initial conditions, originally distributed at random at time $-m$, that fall in the region in the limit $m \to +\infty$. This natural measure is the basis for defining the information dimension d_1 of the strange attractor. For a grid of boxes of side ϵ covering the strange attractor, let p_i be the non-zero natural measure of the ith box. The information dimension of the attractor is then defined (9) to be

$$d_1 = -\lim_{\epsilon \to 0} \frac{\sum_{i=1}^{N(\epsilon)} p_i \log p_i}{\log \epsilon} \qquad (5)$$

where $N(\epsilon)$ is the number of boxes of side ϵ with non-zero measure. In practice, d_1 is usually estimated as the slope of a plot, over a range of small ϵ, of the information sum in the numerator of Eq. 5 versus the logarithm of ϵ. Note that because d_1 is defined in terms of the natural measure of different parts of the attractor, it is not particularly sensitive to miscounting or missing extremely low probability boxes. For experimental purposes, this makes it superior to the usual box-counting dimension d_0, which considers all boxes, containing any amount of natural measure, equally. The relationship between various fractal dimensions is detailed in (*10*).

A dynamical quantity, the Lyapunov dimension for the strange attractor of Eq. 1 is given in terms of the Lyapunov exponents of Eqs. 3a and 4 by the Kaplan-Yorke formula (*10, 11*):

$$d_L = 1 + \frac{\log \lambda_1}{|\log \lambda_2|} \qquad (6)$$

A theorem due to Ledrappier and Young (*12*) states that for random maps, under very general conditions, $d_L = d_1$, and provides a strong link between the important dynamical properties of the system, which can be viewed as the physics of the process, and the static geometric properties of the fractal produced by the system.

Experimental system. Incompressible fluid flows are usually considered incapable of producing fractal concentrations of passively convected tracers, because the incompressibility condition on the fluid velocity, $\nabla \cdot \mathbf{v} = 0$, prevents an initial volume of tracers convected with the fluid velocity $\mathbf{v}$, from achieving a zero volume by following the flow (*13–15*). If, however, the tracers are particles floating on the fluid surface, they respond only to the fluid flow in the surface, and not to the flow normal to the surface. Denoting the fluid surface by $z = 0$, and the coordinates in the surface by (x,y), we see that the flow in the surface can be compressible even though $\nabla \cdot \mathbf{v} = 0$. In particular, $[\partial v_x/\partial x + \partial v_y/\partial z]|_{z=0} = -\partial v_z/\partial z|_{z=0} \neq 0$, and a dissipative two-dimensional flow is possible. Recent theoretical work suggests that surface flows with complicated time dependence could be treated with the theory of random maps (*16, 17*). As a result, it has been argued (*17*) that in many diverse physical situations, particles floating on the surface of a fluid in irregular large-scale motion may assume a fractal distribution.

Our apparatus for investigating this possibility experimentally is shown schematically in Fig. 1. The bulk flow is produced by pumping the working fluid (sucrose solution with specific gravity of about 1.2) over an annular sill, and recovering it from the center of the enclosed basin. With perfect symmetry, steady pumping producing a steady flow would lead to convergence of any passive tracer confined to the surface (a floater) at a point above the fluid recovery port. However, fluid instabilities produce recirculation cells on the surface of the fluid. Steady pumping producing a steady flow in reality would drive passive floaters onto one or more closed curves or fixed points [the Poincaré-Bendixon theorem precludes a steady two-dimensional vector field from producing a strange attractor (*18*)]. Instead, we pump the fluid in a sequence of equally energetic pulses (that is, for the same interval and at the same speed), allowing the fluid to come to rest between pulses. This iterative process takes each point in a two-dimensional region (the stationary fluid surface) and maps it onto another point on the same surface. Thus, the pumping action produces a physical analog to the mathematical system of Eq. 1. The fluid instabilities and other perturbing factors make each pulse different in detail from all of the others, although they are statistically identical. In particular, the axis of the nascent recirculation structure changes randomly from iteration to iteration. Thus we treat the physical system as an approximation to the random map version of Eq. 1. We can control the pumping rate and interval, the viscosity of the working fluid (by controlling its temperature), and the height of the fluid surface above the sill.

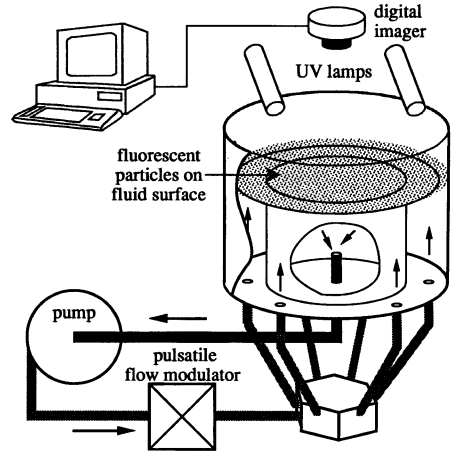

Fig. 1. Schematic of experimental setup. Sucrose solution flows upward in outer cylinder, across the annular sill and downward into recovery basin. The experimental flow is pulsed, adding inertial effects to fluid instabilities. Optical baffling prevents visible specular reflections of ultraviolet lamps from entering camera field of view.

As a physical surrogate for a probability distribution of initial conditions, we use small fluorescent particles (4-μm plastic spheres of specific gravity about 1.05; Duke Scientific 35) that are constrained to the fluid surface by a combination of buoyancy and surface tension. These are initially distributed approximately uniformly (and with a fractional coverage area of about 1 percent) over the fluid surface. A sequence of pumping pulses produces a complicated aggregate pattern of particles, which is visualized by exciting the fluorescent dye in the spheres with ultraviolet light and imaging the distribution of particles with a charge-coupled device camera (Kodak KAF1400 CCD: 1317 × 1035 pixels with 12-bit intensity resolution; each pixel optically subtends an approximately square area 110 μm on a side at the fluid surface). Tests with known quantities of particles distributed uniformly confirm that the intensity of light measured in a given camera pixel is proportional to the number of particles on the optically subtended fluid surface. Normalizing the spatially integrated light intensity allows translation of the gray level in a pixel to a probability value. Typical large-time particle distributions for a particular set of flow parameters are shown in Fig. 2.

Measurement of information dimension. We measure the information dimension of the particle distribution as follows. Using the pixel lattice imposed by the CCD camera as the ϵ-grid discussed above, we calculate the information sum in Eq. 5 for a sequence of square box sizes: 1 pixel × 1 pixel, 2 pixels × 2 pixels, . . ., 128 pixels × 128 pixels. An estimate of the error in

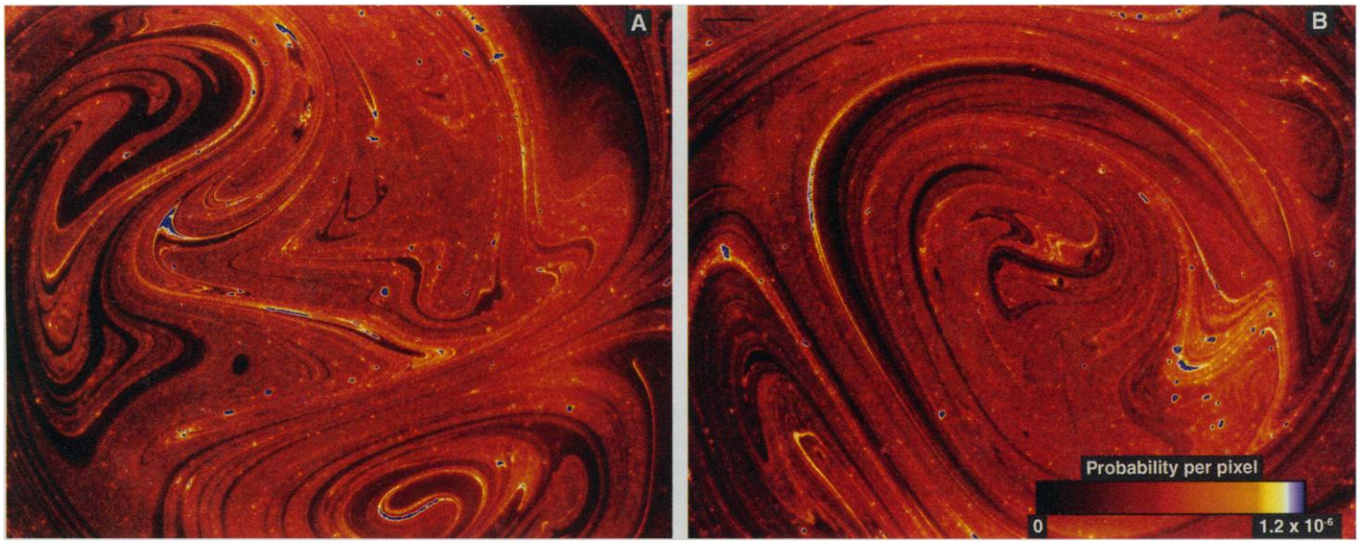

Fig. 2. Radiometrically inferred distribution of tracer particles after experiment has settled into steady-state behavior (**A**). (**B**) corresponds to iterations $n = 25$ and $n = 35$, respectively, in Fig. 5. The particle distributions differ in detail at each iteration, but retain the same information dimension. Black bar in (B) is 5 mm. False color scale indicates range of p_i in Eq. 5 for ϵ equal to one pixel (~100 μm), running from 0 (black) to 1.2×10^{-6} (blue).

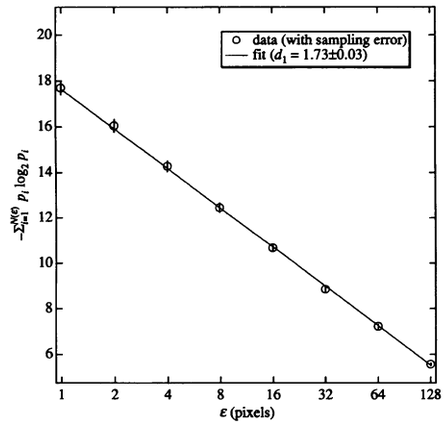

Fig. 3. Typical scaling of the information sum (numerator in Eq. 5) as box side length ϵ is varied. The power-law relationship extending over two orders of magnitude justifies approximating the particle aggregate as a fractal. The slope of the scaling line gives the fractal dimension, $d_1 = 1.73 \pm 0.03$, which is statistically distinct from nearest integer (base-2 logarithms are used on both axes). These data correspond to the particle distribution shown in Fig. 2A.

the information sum was obtained at each box size by using a subset of the entire image as the sampled measure, and randomly shifting the origin of the grid to calculate new values of the information sum. The scatter in these values was used to estimate the error at the corresponding box size. This is probably an overestimate, because the image subsets had fewer boxes of a given size than the full image, and less averaging took place in the sum. The information dimension was estimated as the magnitude of the best-fit slope of a plot of information sum versus logϵ; the standard error in the slope parameter was taken as the uncertainty in the information dimension.

The results of this analysis for the particle distribution in Fig. 2A are shown in Fig. 3. The information sum shows linear scaling over more than two orders of magnitude in grid size. The measured fractal dimension is 1.73 ± 0.03. The statistically significant departure from the integer 2, together with the large scaling range, justifies the interpretation of the particle distribution as an approximate or physical fractal. The information dimension of the particle distribution stabilizes within a few dozen iterates, although the individual particle distributions are completely different in detail. This in itself is evidence that the fractal dimension contains dynamical information.

We note that Fig. 2, which shows some light entering most camera pixels, seems to be at odds with our earlier statement that a strange attractor should have zero area. Several factors contribute to this observation. First, the tracer particles approximating the probability mass do take up finite area; we can only hope for self-similarity over a range of length scales (all much longer than the particle size). Second, the finite resolution of the CCD camera precludes any possibility of our data showing zero-area characteristics. Finally, it is possible to have strange attractors with integral box-counting dimension (that is, they are area-filling) and smaller, non-integral information dimension (*10*).

Approximation of Lyapunov exponents. Estimating Lyapunov exponents on chaotic attractors via computer evolution of a known mathematical system is usually done with the Jacobian matrix of the map F, evaluated along a typical trajectory. We have no practical way to measure the Jacobian in our experiment, so we use an approximate method based on the geometric interpretation of Lyapunov exponents discussed above. Starting with a particle-free surface at rest, we place small, circular distributions of particles on the fluid surface, image the surface, and pulse the flow once. The previously circular distributions, now approximately elliptical, are imaged again (see Fig. 4). The single-step stretching $L_{\max}^{(i)}$ and area reduction $J^{(i)}$ are measured by comparing thresholded images of the circular distributions with the deformed distributions, using an image-processing program. The single-step stretching $L_{\max}^{(i)}$ is defined as the ratio of the maximum linear dimension of the distorted cloud above threshold to the average diameter of the original circular distribution. The area reduction $J^{(i)}$ is defined as the ratio of the number of pixels above threshold in the distorted cloud to the number of pixels above threshold in the original circular distribution. After imaging, the deformed distributions are removed with suction and replaced with new, circular distributions, and the process is repeated.

The stretching $L_{\max}^{(i)}$ is not exactly what is needed to estimate the largest Lyapunov exponent, because, on a given iterate, the direction of maximum stretching is not necessarily along the unstable manifold of the fiducial point at the center of the original particle distribution. We assume that on a given iterate the unstable manifold is oriented at random to the direction of maximum stretching. We estimate a single-step contribution $L_1^{(i)}$ to the overall n-iterate stretching L_1^n, by taking a randomly oriented radius of an ellipse of semimajor

axis $L^{(i)}_{max}$ and semiminor axis $J^{(i)}/L^{(i)}_{max}$. After n iterations the largest Lyapunov exponent λ_1, the dissipation α and their respective uncertainties are then estimated as

$$\lambda_1 \approx \frac{1}{n} \ln L_1^n \approx \frac{1}{n} \ln \prod_{i=1}^{n} L_1^{(i)} \quad (7a)$$

$$\delta\lambda_1 = \frac{1}{\sqrt{n-1}} \sigma(\ln L_1^{(i)}) \quad (7b)$$

and

$$\alpha \approx \frac{1}{n} \ln \prod_{i=1}^{n} J^{(i)} \quad (8a)$$

$$\delta\alpha = \frac{1}{\sqrt{n-1}} \sigma(\ln J^{(i)}) \quad (8b)$$

where the σ's are the sample standard deviations of the quantities in parentheses. This approximate procedure has been tested numerically on analytical maps with strange attractors of approximately the same information dimension as those produced experimentally [the Ikeda-Hammel-Jones-Maloney map (*19*)], and has been shown to produce good results.

The Lyapunov dimension of the experimental attractor was estimated (with n = 105 iterations) by substituting Eq. 4 into the Kaplan-Yorke formula (Eq. 6), with the experimental estimates of the largest Lyapunov exponent and the dissipation given by Eqs. 7a and 8a. The uncertainty in the Lyapunov dimension was calculated with propagation of errors in the modified Kaplan-Yorke formula and the estimated uncertainties given by Eqs. 7b and 8b.

Comparison of information and Lyapunov dimensions. In Fig. 5, we show the dynamical evolution of the measured value of the information dimension of the fluorescent particle distribution for a typical set of flow parameters. The fractal dimension of the particle distribution starts at 2, as expected for a smooth two-dimensional distribution. After relatively few iterations the measured d_1 has dropped to a value less than, and statistically distinct from, the integer 2. The fractal dimension measurement stabilizes around 1.73. Also shown in Fig. 5 is the confidence interval for the Lyapunov dimension (d_L = 1.74 ± 0.02) for the same flow parameters, calculated from the dynamics of the flow as discussed above. The consistency of these quantities supports the idea that the static geometry of the fractal contains information about the dynamics of the underlying process.

Conclusion. We have shown that, at least under some circumstances, the fractal dimension of a physically observed object quantitatively reflects the physical process that produced it. This observation supports continued investigation of fractal characterizations in physics. Although our work provides no general prescription for obtaining predictions of fractal dimensions for arbitrary physical phenomena, the diversity of the phenomena in which fractal characterizations have been obtained argues against any such general prescription. However, we can make the following observation: our modeling has been at a relatively high level of abstraction, focusing on generic local dynamics, rather than on, for example, the Navier Stokes equations themselves. The success of this approach suggests that the connection between dimension and physics may require use of unconventional measures of the physical process, such as Lyapunov exponents.

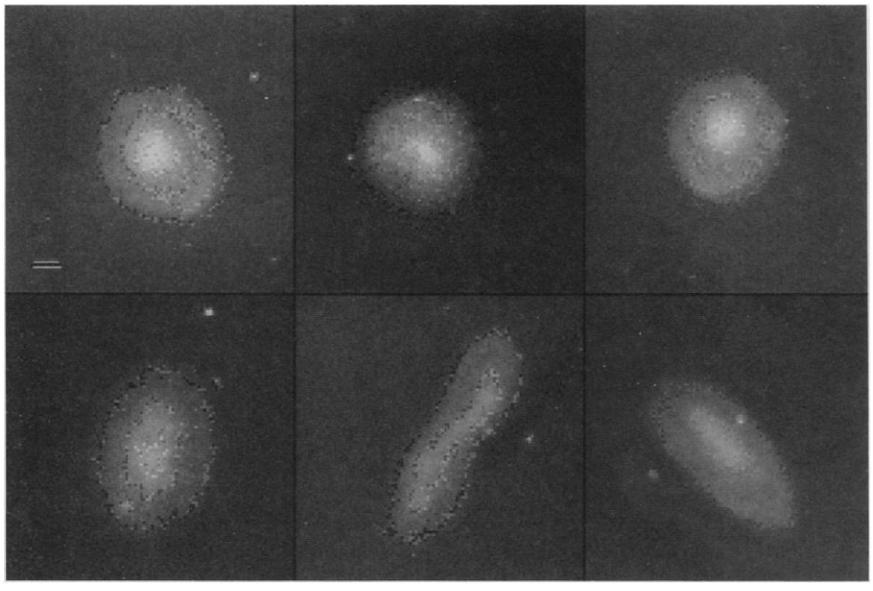

Fig. 4. Initial small, circular particle distributions (top row) are distorted (bottom row) after one interval of pumping (one iteration of the mapping in Eq. 1). Measurement of the distortion allows approximation of Lyapunov exponents for the system of Eq. 1, which is used to model the surface flow. Small bar in top left panel is 1 mm.

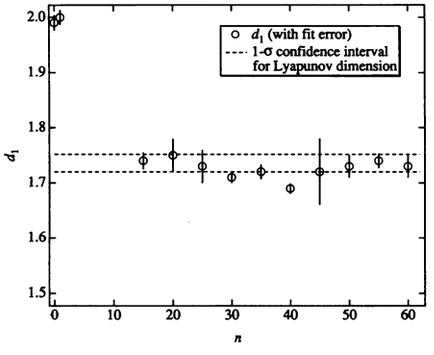

Fig. 5. Measured information dimension of particle aggregate at different time steps n in the random map model. Iterates from n = 2 to n = 14 are not shown, because the particle distributions for those times do not evidence good scaling properties characteristic of fractals; the fractal approximation is not yet satisfied up to the resolution of the experimental system for these values of n. This is not inconsistent with the random map model, which applies to large values of n. Dotted lines show the one standard deviation confidence interval for the Lyapunov dimension predicted from the local dynamics of the surface flow. Consistency with the asymptotic information dimension supports the random map model of the flow, and connects the measured fractal dimension with the physics of the formative process.

REFERENCES AND NOTES

1. B. B. Mandelbrot, *The Fractal Geometry of Nature* (Freeman, New York, 1983).
2. J. Feder, *Fractals* (Plenum, New York, 1988).
3. M. Fleischmann, D. J. Tildesly, R. C. Ball, Eds., *Fractals in the Natural Sciences* (Princeton Univ. Press, Princeton, NJ, 1989).
4. F. Family and T. Vicsek, Eds., *Dynamics of Fractal Surfaces* (World Scientific, Singapore, 1991).
5. Notable exceptions are described in H. G. E. Hentschel and I. Procaccia, *Phys. Rev.* **A29**, 1461 (1984) [clouds]; T. M. Shaw, *Phys. Rev. Lett.* **59**, 1671 (1987) [percolation]; K. R. Sreenivasan, R. Ramshankar, C. Menveau, *Proc. R. Soc. London Ser.* **A 421**, 79 (1989) [isoscalar contours in turbulence]; and P. Constantin, I. Procaccia, K. R. Sreenivasan, *Phys. Rev. Lett.* **67**, 1739 (1991) [isoscalar contours in turbulence]. These papers discuss the theoretical prediction of a fractal dimension that is universal for a category of physical phenomena. In this article, we will be interested in predicting the dimensions of particular fractals, which may differ from case to case.
6. L. P. Kadanoff, *Physics Today,* **39**, 6 (February 1986).
7. D. Ruelle, *Chance and Chaos* (Princeton Univ. Press, Princeton, NJ, 1991), p. 178.
8. _____, *Proc. R. Soc. London Ser.* **A 427**, 241 (1990).
9. P. Grassberger and I. Procaccia, *Phys. Rev. Lett.* **50**, 346 (1983).
10. J. D. Farmer, E. Ott, J. A. Yorke, *Physica* **7D**, 153 (1983).
11. J. Kaplan and J. A. Yorke, in *Lecture Notes in*

Mathematics, H. O. Peitgen and H. O. Walther, Eds. (Springer-Verlag, Berlin, 1978), vol. 730, p. 228.
12. F. Ledrappier and L.-S. Young, *Commun. Math. Phys.* **117**, 529 (1988).
13. J. M. Ottino, C.-W. Leong, H. Rising, P. D. Swanson, *Nature* **333**, 419 (1988).
14. E. Ott and T. M. Antonsen, Jr., *Phys. Rev.* A 39, 3660 (1989).
15. J. M. Ottino *et al.*, *Science* **257**, 754 (1992).
16. L. Yu, E. Ott, Q. Chen, *Phys. Rev. Lett.* **65**, 2935 (1990).
17. _____, *Physica* **53D**, 102 (1991).
18. M. W. Hirsch and S. Smale, *Differential Equations, Dynamical Systems, and Linear Algebra* (Academic Press, Orlando, FL, 1974), chap. 11.
19. S. M. Hammel, C. K. R. T. Jones, J. V. Maloney, *J. Opt. Soc. Am.* **B2**, 552 (1985).

20. We thank C. Howard Hoshall for experimental assistance, and Q. E. Dolecek and P. Q. H. Jensen for assistance with the imaging. Supported by the Department of the Navy, Space and Naval Warfare Systems Command, under contract N00039-91-C-0001 (J.C.S.) and by the Office of Naval Research, Physics Division (E.O.).

17 September 1992; accepted 15 December 1992